A&A 553, A51 (2013)
DOI: 10.1051/0004-6361/201220809

Astronomy & Astrophysics

The *s*-process in the Galactic halo: the fifth signature of spinstars in the early Universe?⋆

G. Cescutti[1], C. Chiappini[1], R. Hirschi[2,3], G. Meynet[4], and U. Frischknecht[2,5]

[1] Leibniz–Institut für Astrophysik Potsdam, An der Sternwarte 16, 14482 Potsdam, Germany
e-mail: cescutti@aip.de
[2] Astrophysics Group, Lennard–Jones Laboratories, EPSAM, Keele University, ST5 5BG, Staffordshire, UK
[3] Kavli Institute for the Physics and Mathematics of the Universe, University of Tokyo, 5-1-5 Kashiwanoha, 277-8583 Kashiwa, Japan
[4] Geneva Observatory, Geneva University, 1290 Sauverny, Switzerland
[5] Department of Physics, University of Basel, Klingelbergstrasse 82, 4056 Basel, Switzerland

Received 28 November 2012 / Accepted 18 February 2013

ABSTRACT

Context. Very old halo stars have previously been found to show at least four different abundance anomalies, which models of fast-rotating massive stars (spinstars) can successfully account for: rise of N/O and C/O, low $^{12}C/^{13}C$, and a primary-like evolution of Be and B. Here we show the impact of these same stars in the enrichment of Sr and Ba in the early Universe.
Aims. We study whether the *s*-process production of fast-rotating massive stars can offer an explanation for the observed spread in [Sr/Ba] ratio in halo stars with metallicity [Fe/H] < -2.5.
Methods. By means of a chemical inhomogeneous model, we computed the enrichment of Sr and Ba by massive stars in the Galactic halo. Our model takes, for the first time, the contribution of spinstars into account.
Results. The model (combining an *r*-process contribution with an *s*-process from fast-rotating massive stars) is able to reproduce the observed scatter in the [Sr/Ba] ratio at [Fe/H] < -2.5. Toward higher metallicities, the stochasticity of the star formation fades away owing to the increasing number of exploding and enriching stars, and as a consequence the predicted scatter decreases.
Conclusions. Our scenario is again based on the existence of spinstars in the early Universe. Very old halo stars have previously been found to show at least four other abundance anomalies, which rotating models of massive stars can successfully account for. Our results provide a fifth independent signature of fast-rotating massive stars: an early enrichment of the Universe in *s*-process elements.

Key words. Galaxy: evolution – Galaxy: halo – stars: rotation – nuclear reactions, nucleosynthesis, abundances – stars: massive – stars: abundances

1. Introduction

Soon after the Big Bang, the appearance of the first stellar generations drastically changed the course of the history of the Universe by enriching the primordial gas with elements heavier than helium (referred to as metals) through both stellar winds and supernova explosions. High-resolution hydrodynamical simulations of the formation of the first stars suggest that these objects have formed in dark matter mini-halos and have played a key role in the formation and properties of the first galaxies (see Karlsson et al. 2011, for a review). One of the key questions that drive enormous theoretical and observational efforts is whether the primordial environment in which the first stars were born made them different from present-day stars. The answer to this question is crucial for understanding the impact of the first stars, in terms both of metal injection and energetic feedback, on the formation of the first galaxies (Bromm & Yoshida 2011). Major endeavors, such as the *James Webb* Space Telescope or the 40 m European Extremely Large Telescope, expected to detect the first galaxies, have been pushing the frontiers of high-resolution hydro-dynamical simulations with the aim of predicting their luminosities and colors (Joggerst & Whalen 2011). These predictions, however, strongly depend on the properties of the first stars, including their mass spectrum and chemical composition.

To simulate the formation of the first stars is technically very challenging, because one starts from large-scale cosmological simulations ($>10^8$ pc) that are then zoomed into the highest density peaks ($<10^{-4}$ pc), covering a dynamical range of at least 10^{12}. When the resolution of these simulations increases, the conclusions in this (still emerging) field change drastically. The best example is the predicted mass spectrum of the first stars: while most of the theoretical simulations predicted that primordial stars were predominantly massive (Bromm et al. 1999; Abel et al. 2002; Bromm & Larson 2004), current results suggest that their mass is in the more normal range for massive stars (between 10 and at most 50 $M_\odot$) and that even low-mass stars could also have formed in the very early Universe (Stacy et al. 2011, 2013; Clark et al. 2011; Greif et al. 2011, 2012).

These state-of-the art simulations have become sophisticated, and are now able to resolve the accretion disk onto the protostellar core. However, the effects of turbulence, magnetic fields and negative feedback by the forming protostar HII region are complex, leading to large model uncertainties. Moreover, an enormous resolution is needed to correctly follow the accretion process (see Ferrara 2012, for a recent discussion). As a consequence, the current mass spectrum of the first stars is still not known. Very interestingly, the most recent simulations seem to converge to one result: there is sufficient angular momentum in

⋆ Appendix A is available in electronic form at http://www.aanda.org

the protocloud collapse to yield rapidly rotating stars near the break-up speeds (e.g. Stacy et al. 2011, 2013). As we see below, the completely independent approach of Galactic Archaeology, had already pointed in the same direction.

It is now recognized that Galactic Archaeology offers a powerful alternative way of probing the nature of the first stellar generations (Freeman & Bland-Hawthorn 2002; Bromm & Yoshida 2011; Tumlinson 2010), thus providing invaluable constraints to the above-mentioned simulations. It is in the Milky Way (MW) and its satellites that the oldest and most metal-poor stars in the Universe are observable, because they were born at times or equivalent redshifts that are still out of reach of even the deepest planned extragalactic surveys.

Low-mass stars (masses below 80% of a solar mass) have comparable lifetimes to the age of the Universe. We, therefore, expect that in their atmospheres, the elemental abundances of the gas at the time of their birth are mostly preserved, offering a local benchmark to cosmology. These stars thus keep memory of the unique nucleosynthesis in the first stellar generations, thereby providing invaluable constraints on the masses of the first stars, hence on their stellar yields. This is the very basic input for modeling subsequent stellar generations, leading to the abundance distribution prevailing at present time.

Reliable age determination, especially for the oldest stars, has been one of the biggest challenges in astronomy, although a breakthrough is expected to come from astroseismology (Chiappini 2012). In some rare cases it was possible to estimate an age by measuring long-lived radioactive elements such as Th and U (Cayrel et al. 2001), albeit with still non-negligible uncertainties. In the meantime, the strategy adopted so far has been to look for the most metal-poor stars in the MW and its satellites, both presumably formed from a gas enriched only by a few first supernovae.

The hunt for the most metal-poor stars in the Universe is not an easy task. This search is restricted to nearby (resolved) stellar populations: the MW halo and its satellites. The chemically most primitive stars are extremely rare. Despite their scarcity, in the MW halo around 130 halo stars, with metallicities below [Fe/H] = −3, are currently known (Frebel 2010, for a recent review). Only two of them have [Fe/H] < −5 (Frebel et al. 2005, 2008; Christlieb et al. 2002), while more recently, Caffau et al. (2011) has discovered a star with an [Fe/H] = −4.89 (so slightly above −5) but with the lowest global metallicity ($Z \leq 7.4\times10^{-7}$) not enhanced in C and N differently from the Frebel and the Christlieb stars.

Recently, another window into the very metal-poor universe has been provided by the discovery of the so-called ultra-faint dwarf spheroidal galaxies. These objects are dominated by dark matter and have very low average metallicities (some show a mean [Fe/H] ∼ −2.6), thus offering an excellent environment in which to search for more fossil records of the early enrichment. The search for more of these Rosetta stones in the history of the Universe constitutes the goal of several planned and ongoing surveys, and for details the interested reader is referred to SEGUE (Yanny et al. 2009), APOGEE (Eisenstein et al. 2011), LAMOST (Zhao et al. 2006), SkyMapper (Keller et al. 2007), 4MOST (de Jong et al. 2012), and WEAVE (Balcells et al. 2010).

The new information on cosmic abundances provided by the still modest samples of very metal-poor stars in the halo (still confined to mostly nearby and brighter objects) and the MW satellites have already proven to be a rich source of information on the nature of the first stellar generations. In their pioneering work, Cayrel et al. (2004) derived abundances of several elements for a fairly large sample of very metal-poor normal stars (not C-enhanced), obtained with the ESO Large Program "First Stars". Their data of unprecedented quality reveals a striking homogeneity in the chemical properties of halo stars.

At first sight, this uniformity was interpreted as a challenge to the view that the whole Galactic halo formed from the successive swallowing of smaller stellar systems with independent evolutionary histories, as predicted from the cold dark matter theory. The situation turned out to be more complex, since the same stars were found to show large scatter in *r*- and *s*-process elements (François et al. 2007) and in the N/O ratios (Spite et al. 2005).

The first stars are believed to have been radically different from present-day massive stars, because they were metal-free. The lack (or only traces) of metals leads to faster surface rotation velocities, since metal-poor stars are more compact than metal-rich ones. Stars formed from a gas whose global metallicity is below ∼1/2000 that of the Sun (i.e. $Z = 10^{-5}$) could attain rotational velocities of 500–800 km s^{-1} (depending on the stellar mass, hereafter called spinstars – see Maeder & Meynet 2012, for a recent review).

Two important effects of interest for the present work arise in spinstars:

a) rotation triggers mixing processes inside the star, which leads to producing large quantities of primary ^{14}N, ^{13}C and ^{22}Ne (Meynet et al. 2008, and references therein). The production of primary ^{22}Ne has a strong impact on the *s*-process nucleosynthesis in spinstars compared to nonrotating stars, increasing the *s*-process yields of heavy elements by orders of magnitude (e.g. Pignatari et al. 2008; Chiappini et al. 2011; Frischknecht et al. 2012);
b) the strong mixing caused by rotation enriches the stellar surface, thus increasing the opacity of the outer layer and producing line-driven winds (but see Muijres et al. 2012). In addition, fast rotation can also lead to mechanical mass-loss. Both mechanisms are already able to trigger non-negligible mass loss at very low metallicities (a result not achieved by standard models without rotation).

We have shown that a generation of spinstars in the very early Universe is currently the most promising for the increasing of N/O ratio observed in very metal-poor normal stars in the Galactic halo (Chiappini et al. 2006). Indeed, asymptotic giant branch stars (AGBs), that produce ^{14}N and ^{13}C efficiently, have not had time to contribute to the chemical enrichment of the early Universe due to their long lifetimes; another viable explanation not fully explored yet is the contribution of SAGB. Our models with spinstars also naturally account for the observed increase in the C/O ratio in halo stars towards low metallicities (Chiappini et al. 2006; Fabbian et al. 2009). Moreover, if spinstars were common phenomena in the early Universe, the metal-poor ISM of galaxies with a star formation history similar to the one inferred for our Galactic halo, should have ^{12}C/^{13}C ratios between 30–300 below [Fe/H] = −3. Without fast rotators, the predicted ^{12}C/^{13}C ratios is 4500 at [Fe/H] = −3.5 increasing to 31 000 at [Fe/H] = −5.0 (Chiappini et al. 2008). Current observations of this isotopic ratio in very metal-poor giant stars in the Galactic halo (Spite et al. 2006) agree better with chemical evolution models that include fast rotators. Recently, the same results for C isotopes and for the ratio N/O have been obtained in Kobayashi et al. (2011) using another chemical model.

To test the last predictions, challenging measurements of the ^{12}C/^{13}C in more extremely metal-poor giants or turnoff stars are required (only feasible with 30 m-class telescopes). Furthermore, we explain the apparently contradictory finding of

a large scatter in C, N and the almost complete lack of scatter in [α/Fe] ratios of the same stars as being the consequence of the combination of a stochastic star formation rate in the early universe (hence, incomplete sampling of the IMF and incomplete halo mixing), coupled with a strong yield dependence on the stellar mass for these particular elements (Cescutti & Chiappini 2010): spinstars provide a nucleosynthetic site in which the yields of C, N strongly depend on stellar mass.

In summary, we claim that the rise in N/O and C/O and the low $^{12}C/^{13}C$ in very metal-poor halo stars are three footprints of the existence of spinstars in the earliest phases of the Universe. A fourth signature has recently been suggested by Prantzos (2012) who argues that the observed primary-like evolution of Be and B can be explained if galactic cosmic rays are accelerated from the wind material of rotating massive stars, rich in CNO, hit by the forward shock of the subsequent supernova explosions. These four footprints have been found in the very metal-poor Universe ([Fe/H] < -3).

In the present paper we suggest that two puzzling results involving n-capture elements, such as Y, Sr, and Ba, might again point to the existence of spinstars in the early Universe, namely:

- The large scatter in the abundance ratios of *s*-process elements from the first and second peaks, e.g., [Sr/Ba] (see Sect. 2), which cannot be explained even by inhomogeneous models that otherwise match the lack of scatter in α-elements, and the large scatter of the same elements with respect to iron (e.g., Sr and Ba in Cescutti 2008);
- The large enhancements of Ba, La, Y, and Sr found in stars of NGC 6522, a bulge globular cluster shown to be the oldest one in the MW (Barbuy et al. 2009; Chiappini et al. 2011).

Indeed, Chiappini et al. (2011) have shown that a) the scatter in the [Sr/Ba] and [Y/Ba] for very metal-poor halo stars is similar to what is found in the NGC 6522 stars; and b) that the enrichment of Sr, Y, Ba, and La in five out of eight stars of NGC 6522 could be either the *s*-process activation in early generations of spinstars or the *s*-process due to the contamination from a low-mass AGB stars in a binary system, with initial metallicity coincident with the metal content of the cluster. In the first case, the chemical enrichment is from stars polluting the primordial material before forming the cluster, whereas in the second the chemical enrichment would happen via AGB-mass transfer at whatever point in the history of NGC 6522, thus polluting the stars we are now observing. However, the remaining three stars showing the highest [Y/Ba] are not compatible with *s*-process nucleosynthesis in AGB stars and can be readily explained from early enrichment from spinstars. It is now possible to investigate this hypothesis in a more quantitative way by using inhomogenous chemical evolution models computed with the most recent calculations carried out by our group (Frischknecht et al. 2012; in prep.). In the present work, we focus on the observed scatter of [Sr/Fe], [Ba/Fe], and [Sr/Ba] in very metal-poor halo stars. We argue that fast-rotating massive stars have also left a footprint in the early enrichment of heavy elements, such as Sr and Ba. In a forthcoming paper we will then specifically discuss models for the Galactic bulge.

The paper is organized as follows. In Sect. 2 we describe the current situation with respect to the predicted stellar yields of heavy elements and justify the use of empirical yields for the *r*-process. In Sect. 3 the observational data is described. Sections 4 and 5 describe the chemical model and the adopted stellar yields, respectively. In Sect. 5 our results are presented, and in Sect. 6 we summarize our conclusions.

2. The production of heavy elements: an open debate

Elements with $Z > 30$ are labeled neutron capture elements: they are mainly formed through neutron captures, and not through fusion, because charged particle reactions on elements beyond iron ($Z = 26$) are endothermic (omitting the p-process, responsible for less than 1% of the heavy elements). The neutron capture process is split in rapid process (*r*-process) or slow process (*s*-process) depending on whether the timescale for neutron capture τ_n is faster or slower than radioactive beta decay τ_β, according to the initial definition by Burbidge et al. (1957).

There are several sites of production for the *s*-process. Massive stars produce the so-called weak *s*-process ($60 < A < 90$) and intermediate- and low-mass stars produce the main *s*-process (up to lead) – see recent review by Käppeler et al. (2011). For the *r*-process, the final states of massive stars, where extremely high neutron density are achievable, seem to provide a promising site (although still very uncertain, see Thielemann et al. 2011). A multiplicity of hypotheses does exist, such as neutrino winds during SNII (Woosley et al. 1994; Takahashi et al. 1994; Thompson 2003; Arcones et al. 2007; Farouqi et al. 2009), neutron star mergers (Freiburghaus et al. 1999; Goriely et al. 2011; Korobkin et al. 2012), O-Mg-Ne core explosion (Wanajo et al. 2011), asymmetric explosions (Cameron 2003; Arnould et al. 2007), quark novae (Jaikumar et al. 2007), and magnetorotationally driven supernovae (Winteler et al. 2012).

The general complexity of these environments, coupled with the inaccessibility of the nuclear data of the isotopes involved, leads to still uncertain predictions for the stellar yields. Only recently have a few SNII simulations started to successfully explode stellar cores, and the results are still controversial. This is the case for the simulations of O-Mg-Ne core collapse supernovae (SN) by Kitaura et al. (2006) and the nucleosynthesis calculated on this basis by Wanajo et al. (2011, 2009).

Even though the *r*-process is not clearly understood, most recent studies in this field point to massive stars (with the remarkable exception of the neutron star mergers) as the most promising production site. If this is the case, the chemical enrichment timescale of the *r*- and *s*-processes are distinct, namely: a few tens of million years for the *r*-process nuclei (typical lifetime for a massive star), and more than 0.5 Gyr for the bulk of production of *s*-process in AGB stars (Käppeler et al. 2011). Some production of *s*-process is also expected to take place in massive stars, although the overall contribution is negligible, especially in the very metal-poor regime (see Raiteri et al. 1992). For this reason, it has been common to associate the n-capture elements in the extremely metal-poor (EMP) stars of the halo to *r*-process production, as first pointed out by Truran (1981).

The solar system isotopic abundances (see Grevesse et al. 2010) can be split into *r*- and *s*-process contributions. Theoretically the *s*-process abundance pattern is known, and the solar *s*-process pattern is obtained by scaling to the abundances of isotopes exclusively produced by *s*-process (isotopes shielded against *r*-process by the corresponding stable isobar of $Z - 2$). The *r*-process contribution to the solar system (Arlandini et al. 1999; Simmerer et al. 2004) is determined by subtracting the *s*-process contribution. In this way the so-called *r*-process contribution to the solar system is found, although is not free of theoretical uncertainties in the *s*-process contribution, chemical evolution, or other processes that could be hidden.

Although the relative amount of neutron capture elements is small compared to those of the lighter elements (roughly 10^{-6}), their absorption lines in the stellar spectra can be observed and

their abundances calculated even for the most metal-poor stars. Ever since the work by Sneden et al. (1996, and also Sneden et al. 2003, 2008), remarkable agreement has been found between the abundance pattern from Ba up to Th measured in a very *r*-process-rich EMP star (CS 22892−052) and the *r*-process contribution to the solar system. This appeared to confirm both the theory of the *s*-process from one side and the idea that *r*-process was the only producer of (heavy) neutron capture in the early universe.

On the other hand, the same investigators, Sneden et al. (1996, and also Sneden et al. 2003, 2008), have shown that the pattern for light neutron capture elements (from Sr to Ag) does not always match the so-called *r*-process solar pattern and Wasserburg et al. (1996) have invoked two *r*-processes to explain radioactive isotopes anomalies in solar meteorites. Moreover, the ratio of light to heavy neutron capture elements in other EMP stars is not constant, as expected for two species coming from the same process. The light elements are more enriched in some EMP compared to the expectations of a pure *r*-process pattern, and show an increasing scatter towards low metallicities, up to [Fe/H] ~ -4 (Honda et al. 2004; François et al. 2007).

A new process was invoked to provide the additional contribution for light neutron capture elements and, at the same time, possibly produce the spread in the ratio of light to heavy neutron capture elements. Travaglio et al. (2004) call this process the lighter element primary process (LEPP), without specifying a possible *r*- or *s*-origin (although typically *s*-processes are not a primary process). Later, when analyzing the pattern of this possible missing process, Montes et al. (2007) obtained two viable solutions, one with typical neutron fluxes of the *r*-process and the other closer to *s*-process values, both of them able to provide roughly the correct pattern.

For the first time, it was shown in the work by Pignatari et al. (2008), who assume a primary amount of ^{22}Ne guided by rotating models, that rotating massive stars could produce a significant amount of s process at low *Z*. More recently, Frischknecht et al. (2012) have calculated full stellar evolution models using an extended nuclear reaction network and show that fast rotation can boost the production of *s*-process at low metallicities.

Here our goal is to test the impact of these yields in the early chemical enrichment of the Galaxy. Clearly, the *s*-process in fast-rotating massive stars will not be the only contributor to the Ba and Sr in the early Universe, since most of it comes from the still uncertain *r*-process. This means that in our models, we need to also include a production via *r*-process. Unfortunately, given the uncertainties discussed before, only a few groups provide *r*-process stellar yields: for neutrino wind models (Arcones & Montes 2011) and for O-Ne-Mg core collapse models (Wanajo et al. 2011). However, as recently shown by Hansen et al. (2013) for the case of Sr, these predictions can still vary by more than 3 dex, and although the models quoted above do produce Sr, they do not produce Ba. Other processes, more promising for Ba production, such as neutron star merging or magneto-rotationally driven SN have not yet led to detailed stellar yield computations.

In the present work we follow an alternative way to deal with the problem of the absence of robust theoretical yield predictions for the *r*-process, already adopted by other authors such as Travaglio et al. (1999, 2004), Ishimaru & Wanajo (1999), and Cescutti et al. (2006): we adopt empirical yields, which are extracted from the available observational constraints (see Sect. 4.2.1). It turns out that the empirical yields we estimate are within the uncertainties of the present *r*-process models. This will enable us to quantitatively estimate the impact of spinstars on the early enrichment of heavy elements, as well as to guide theoretical efforts on *r*-process nucleosynthesis.

3. Observational data

3.1. Metallicity distribution function

The chemical evolution model assumptions on star formation history and winds are such that the overall shape of the metallicity distribution (MDF) of the halo stars is reproduced. The MDF is strongly affected by the selection criteria of each sample, and most studies have tried to take this into account. A comparison with the results by Yong et al. (2013), who focus on the extremely metal-poor tail of the MDF, shows good agreement with the theoretical predictions of Cescutti & Chiappini (2010), which is essentially the same model as is adopted here (see Fig. 3 of Yong et al. 2013).

Two other recent analyses making use of data from the Hamburg/ESO objective-prism survey (HES) (Christlieb et al. 2008) have been recently carried out with the goal of determining the whole halo MDF: the Schörck et al. (2009) MDF based on metal-poor giants and the MDF from Li et al. (2010) based on main sequence turn off stars (MSTO) stars. Both analyses use statically well understood selection criteria to obtain a large number of metal-poor giants (1638) and metal-poor MSTO stars (617), respectively.

Here we compare our model predictions with the MDF traced by MSTO stars rather than giants, because as shown by Li et al. (2010), the dwarfs are less affected by survey-volume corrections. We are aware that this sample lacks the extremely metal-poor tail of stars with [Fe/H] < -3.5, but larger statistically complete samples are required for this purpose. Fortunately, such samples will be obtained from much larger and deeper surveys in the near future, such as from SEGUE-2, LAMOST, SkyMapper, and 4MOST.

3.2. Chemical abundances

We have adopted observational abundance ratios from the literature; the data for the neutron capture elements and for the α-elements are those collected by Frebel (2010)[1], labeled as halo stars[2]. Among the halo stars collected, we differentiate the normal stars from the carbon-enhanced metal-poor (CEMP) stars. Around 20% of stars with [Fe/H] < -2.0 are CEMP stars (Lucatello et al. 2006). We follow the definition given by Masseron et al. (2010) where a CEMP star is defined as having [C/Fe] > 0.9. The latter can be subclassified as (see Masseron et al. 2010), based on Ba and Eu, namely:

- CEMP-s: [Ba/Fe] > 1 and [Ba/Eu] > 0
- CEMP-rs [Eu/Fe] > 1 and [Ba/Eu] > 0
- CEMP-no [Ba/Fe] < 1 and no Eu value
- CEMP-r [Ba/Fe] < 1 and [Ba/Eu] < 0
- CEMP-low s [Ba/Fe] < 1 and [Ba/Eu] > 0.

[1] http://cdsarc.u-strasbg.fr/cgi-bin/qcat?J/AN/331/474

[2] The list of the authors we use from the collection are McWilliam et al. (1995), McWilliam (1998), Westin et al. (2000), Aoki et al. (2002), Cowan et al. (2002), Ivans et al. (2003), Honda et al. (2004), Aoki et al. (2005), Barklem et al. (2005), Aoki et al. (2006), Ivans et al. (2006), Masseron et al. (2006), Preston et al. (2006), Aoki et al. (2007), François et al. (2007), Lai et al. (2007), Cohen et al. (2008), Lai et al. (2008), Roederer et al. (2008), Bonifacio et al. (2009), Hayek et al. (2009).

We note that in our sample we have just one CEMP with [Ba/Fe] < 1 with Eu measurement, which is classified as CEMP-*r*, and so the CEMP-low *s* category is missing. For our purposes, the above categories are not strictly necessary, but we prefer to refer to the literature than create "ad hoc" definitions. The important distinction in the present work is between CEMP-(r)s and CEMP-no, hence whether a strong signature of *s*-process is present or not.

Indeed CEMP-s most likely stem from binary mass transfer from a previous AGB companion (Bisterzo et al. 2012; Lugaro et al. 2012), and for this reason CEMP-s do not reflect the chemical evolution of the ISM.

4. The chemical evolution models

Homogeneous chemical evolution models alone cannot take advantage of the precious information recorded in the scatter of key element abundance ratio of old stars, in different environments. The inhomogenous chemical evolution models (i.e. models that relax the instantaneous mixing approximation), in turn, requires a cosmological framework in which it is possible to predict the properties (volumes) of the inhomogeneities arising from both merger building blocks and unmixed ISM (e.g., feedback). However, in this case other uncertainties related to the field of cosmological simulations will play a crucial role in the results. Although we have started to work in this direction, we still think that it is important to develop simpler inhomogenous models, of the kind presented here.

Indeed, these models will serve as a test bench to study the different nucleosynthetic prescriptions proposed by the different scenarios. The goal is to identify key abundance ratios, as well as the most promising stellar yields, to be implemented in cosmological simulations. This step is crucial for avoiding spending unnecessary CPU time with models that do not meet the minimum requirement set by a first comparison with observations.

The neutron capture element spread in EMP stars has already been the subject of other investigations. We recall here the works of Tsujimoto et al. (1999), Ishimaru & Wanajo (1999), Travaglio et al. (2001), Argast et al. (2002, 2004), and Karlsson & Gustafsson (2005). Most of these models reproduced the spread in n-capture elements observed in EMP stars, but left unexplained other problems: a much smaller scatter observed for the other elements (for instance α-elements, see Cayrel et al. 2004; Bonifacio et al. 2012), the reduction of the spread toward higher metallicity for the neutron capture elements, and the large scatter observed in N/O and C/O.

This has pointed to a different solution in which the inhomogeneities arise from a stochastic formation of massive stars. The spread can be generated by the enrichment of different species if they are produced by different ranges of masses, as shown for heavy neutron capture elements as a function of iron in Cescutti (2008); at the same time, the spread is reduced after a few generations of stars, and it is small for elements that share the same range of production (as α-elements and iron). This approach has also been used for the CNO elements (see Cescutti & Chiappini 2010) to investigate the impact of the inhomogenous modeling on the observed spread (in particular, of the ratio N/O) in EMP stars.

Here we consider the same chemical evolution model as adopted in Cescutti & Chiappini (2010), based on the inhomogenous model developed by Cescutti (2008) and on the homogeneous model of Chiappini et al. (2008). We consider that the halo consists of many independent regions, each with the same typical volume, and each region does not interact with the others. We decided to have a typical volume with a radius of roughly 90 pc, and the number of assumed volumes is 100 to ensure good statistical results. The dimension of the volume is large enough to allow us to neglect the interactions among different volumes, at least as a first approximation. In fact, for typical ISM densities, a supernova remnant becomes indistinguishable from the ISM – i.e., merges with the ISM – before reaching ~50 pc (Thornton et al. 1998), less than the size of our region. We do not use larger volumes because we would lose the stochasticity we are looking for; in fact, larger volumes produce more homogeneous results.

In each region, we assume the same law for the infall of the gas with primordial composition, following the homogeneous model by Chiappini et al. (2008), so we have the following Gaussian law:

$$\frac{\mathrm{d}Gas_{\rm in}(t)}{\mathrm{d}t} \propto \mathrm{e}^{-(t-t_{\rm o})^2/\sigma_{\rm o}^2} \quad (1)$$

where $t_{\rm o}$ is set to 100 Myr and $\sigma_{\rm o}$ is 50 Myr. Similarly, the star formation rate (SFR) is defined as

$$SFR(t) \propto (\rho_{\rm gas}(t))^{1.5} \quad (2)$$

where $\rho_{\rm gas}(t)$ is the density of the gas mass inside the considered volume. Moreover, the model takes an outflow from the system into account:

$$\frac{\mathrm{d}Gas_{\rm out}(t)}{\mathrm{d}t} \propto SFR(t). \quad (3)$$

Knowing the mass that is transformed into stars in a timestep (hereafter, $M^{\rm new}_{\rm stars}$), we therefore assign the mass to one star with a random function, weighted according to the initial mass function (IMF) of Scalo (1986) in the range between 0.1 and 100 $M_{\odot}$. Then we extract the mass of another star, and we repeat this cycle until the total mass of newly formed stars exceeds $M^{\rm new}_{\rm stars}$. In this way, in each region at each timestep, the $M^{\rm new}_{\rm stars}$ is the same, but the total number and mass distribution of the stars are different. We then know the mass of each star contained in each region, when it is born, and when it will die, assuming the stellar lifetimes of Maeder & Meynet (1989). At the end of its lifetime, each star enriches the ISM taking the enrichment due to that star into account and owing to the already present mass of each element locked in that star when it was born.

Yields for α-elements and Fe are the same as in François et al. (2004). The model considers the production by *s*-process from 1.5 to 3 $M_{\odot}$ stars and SNIa enrichment, as in Cescutti et al. (2006). The model does not include the most recent and accurate yields for AGB, and the very low-metallicity yields for AGB are extrapolated. However, due to the longer lifetime compared to the halo star formation history, this production is hardly seen in the results of the model for [Fe/H] < -1, as well as in the abundance pattern of normal EMP. Super-AGB stars can also be involved in the production of neutron capture elements, but at the present time yields for those elements from SAGB are not available; however, the production of *s*-process elements in their convective pulses is expected to be small (Siess 2010). Additional studies are required to clarify this aspect.

4.1. First test: reproducing the MDF and the [α/Fe] low scatter

This model is able to reproduce the MDF measured for the halo by Li et al. (2010) based on HES data of main sequence turn-off stars (see Fig. 1). This comparison shows that the timescale of enrichment of the model looks like that of the halo stars in the solar vicinity.

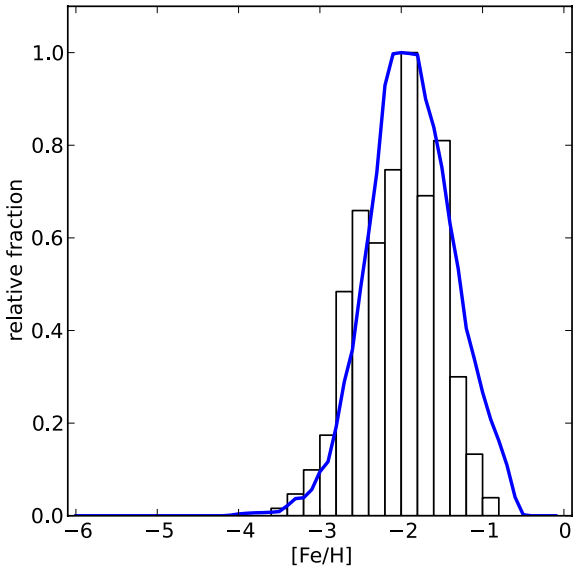

Fig. 1. Comparison between the model MDF in blue line and the observed halo MDF by Li et al. (2010): main-sequence turnoff stars in the HESS (Hamburg ESO) for which [Fe/H] < −1.

In Fig. 2, we show the predictions of our model for the α-elements Ca and Si. Our model predicts a narrow spread for these abundance ratios, which is compatible with the observational data. In addition, our model predictions show a slightly increase in the scatter in the very-metal-poor regime. Interestingly, inhomogenous models, as the one shown here, do predict a few outliers with low values of [α/Fe].

4.2. Stellar yields for heavy elements

4.2.1. Empirical yields for the *r*-process

As mentioned in Sect. 2, the site of production of *r*-process elements is still a matter of debate. In particular, most of the neutron reactions involving *r*-process elements are beyond the reach of nuclear physics experiment. In such a situation, we must use observational data to guide the theoretical models for this process.

Given the above, we adopt here the following approach (see also Cescutti et al. 2006): we compute a homogeneous chemical evolution model where the yields of Ba are chosen so as to reproduce the mean trend of [Ba/Fe] versus [Fe/H] (see Fig. 3). The resulting yields are what we call empirical yields here.

The empirical yields are obtained as the simplest array able to reproduce the observed trend of increasing [Ba/Fe] with metallicity, but also present one important property, namely, the need for two different sites of production (see Fig. 4):

- a strong production in a narrow mass range 8–10 $M_{\odot}$ that we call standard *r*-process site;
- an extended contribution coming from stars with higher masses (from 10 up to 30 $M_{\odot}$), whose contribution is lower by ∼2 dex than that of the standard *r*-process, and which we here denote as the extended *r*-process site.

The standard *r*-process assumptions fit the general concept of *r*-process production, so an intense production in relatively rare events. On the other hand, the extended *r*-process seems a necessary step to explain the presence of stars with [Ba/Fe] ∼ −0.7 at metallicities lower than [Fe/H] ∼ −3.5 (Francois et al. 2007, see Fig. 4). This effect can be appreciated better from the inhomogenous results (see comparison of model results with and without the extended *r*-process in Fig. A.1 in the Appendix), and it is a viable way to explain the absence of stars lacking Sr and Ba (Roederer 2013), as in the case without the extended *r*-process.

We here assume the *r*-process yields of Sr scale with those of Ba. The adopted scaling factor (of 3.16) has been taken from the solar system *r*-process contribution (see Sect. 2) as determined by Simmerer et al. (2004). Another meaningful assumption could have been the choice of the mean observed ratio between Sr and Ba in *r*-process-rich stars (see Cowan et al. 2006). In this case, the Sr/Ba ratio would be around 0.2 dex higher. On the other hand, this same ratio measured in the *r*-process rich star CS22892−052 is close to the value that we have adopted. We stress that we have selected a simple approach here to the *r*-process production, although many authors have recently started to suspect that this assumption may be not completely valid (Roederer et al. 2010; Boyd et al. 2012); on the other hand, our simple approach is reasonable, since the emphasis of this paper is not on the *r*-process issue but on the contribution from spinstars to the production of strontium and barium.

Interestingly the stellar mass range for standard *r*-process is close to the one predicted by theoretical models of ONeMg core supernovae (with initial masses toward the lower end of the massive stars). However, the latest models (Wanajo et al. 2011, 2009) do not succeed in producing heavy neutron capture elements such as Ba. It is also worth mentioning that the stellar mass range $8 < M_{\odot} < 10$ is in the transition between the super AGB stars and the electron capture supernova. For this reason we stress that the final fate of these stars is still rather uncertain (Siess 2007, 2010).

As we see, the role of the extended *r*-process contribution, which we need to consider when empirically explaining the observed [Ba/Fe] and [Sr/Fe] in EMP halo stars, can be replaced by the contribution of spinstars.

4.2.2. The contribution of spinstars

To illustrate the impact of rotating stellar models on the chemical enrichment of Sr and Ba in the earliest phases of the Universe, we now focus on three sets of inhomogeneous chemical evolution models, computed with the following sets of stellar yields (see Fig. 4 and Table 1):

- *r-model*: assume only empirical yields for the *r*-process (standard + extended);
- *as-model*: assume only the standard *r*-process yields (no extended *r*-process contribution), plus the *s*-process yields coming from rotating stellar models (see below);
- *fs-model*: similar to the model above, but with *s*-process yields coming from the *s*-process in fast-rotating stellar (spinstars) models.

The nucleosynthesis adopted in the *as-model* for the *s*-process comes from unpublished results by Frischknecht (2011, Ph.D. Thesis). In this set of yields, the *s*-process for massive stars is computed for $v_{\rm ini}/v_{\rm crit} = 0.4$ and for a standard choice for the reaction ^{17}O(α,γ) from Caughlan & Fowler (1988); they are composed of a grid of four stellar masses (15, 20, 25 and 40 $M_{\odot}$) and three metallicities (solar metallicity, 10^{-3}, 10^{-5}); in Fig. 4 we show the yields for the two lowest metallicity cases. We do not extrapolate the production toward stars that are more massive than 40 $M_{\odot}$ (although it is realistic also to have a production in this range), but we extrapolated the $Z = 10^{-5}$ grid down to $Z = 0$. In addition to the *s*-process in massive stars, we take our empirical *r*-process enrichment into account but coming only from the standard *r*-process site. In this way we are decoupling the sites of

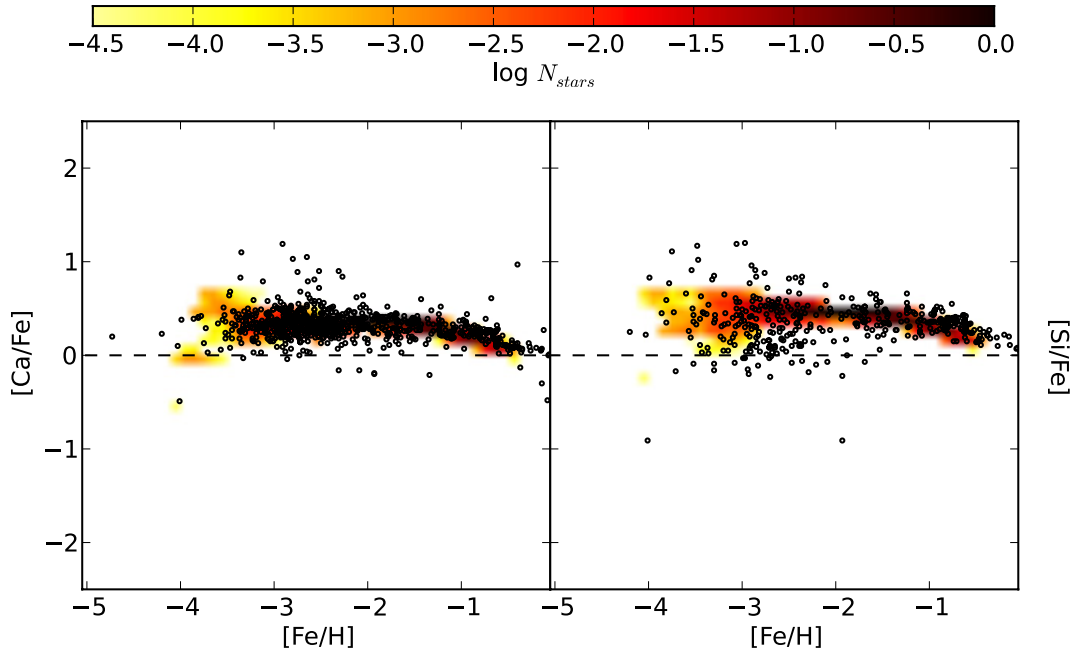

Fig. 2. [Ca/Fe] and [Si/Fe] vs. [Fe/H], from *left to right*. The density plot is the distribution of simulated long-living stars for our model; the density is on a logarithmic scale, normalized to the peak of the distribution and the bar over the plot describes the assumed color scale. Superimposed on the density plot, we show the abundances ratios for halo stars (data from Frebel 2010).

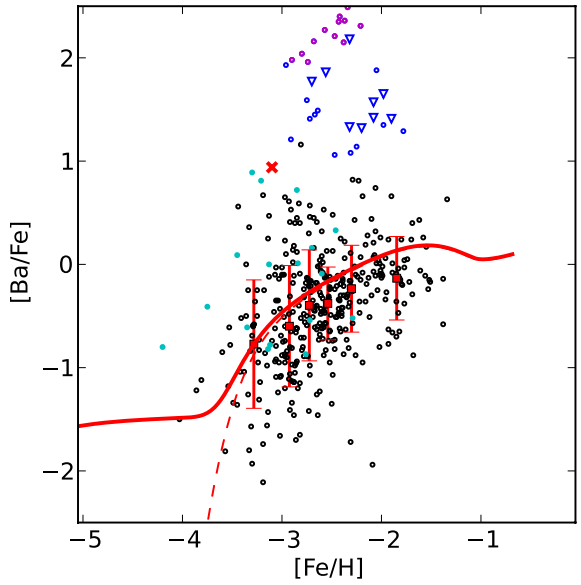

Fig. 3. [Ba/Fe] vs. [Fe/H] abundances ratios of the halo stars (data from Frebel 2010): black open circle are normal stars, blue open circle for CEMP-s stars (open triangles without Eu value) magenta open circle for CEMP-rs, cyan filled circle for CEMP-no, and red × marker for the CEMP-r star. The error bars represent the mean and the standard deviations for the normal stars abundances calculated over different bins in [Fe/H]. The bins are calculated in such a way that each bin contains the same number of data points. The results of the homogenous model with the assumed empirical yields for Ba is shown by the solid line; the dashed line shows the results when only the "standard" *r*-process site is considered.

production for the two processes. Interestingly, this figure shows that the *s*-process of spinstars plays the role here of the extended *r*-process, which is not used in this model.

It is worth pointing out that the yields we have used for the *as-model* are very conservative, among the models computed by Frischknecht et al. (2012) for 25 $M_{\odot}$. In the *fs-model*, we have adopted a more robust production of *s*-process, which is achievable if we consider the *s*-process yields of massive stars computed for $v_{\rm ini}/v_{\rm crit} = 0.5$ (fast rotators) and for a reaction rate $^{17}{\rm O}(\alpha,\gamma)^{21}{\rm Ne}$ one tenth of the standard choice. Indeed, the adopted $v_{\rm ini}/v_{\rm crit} = 0.4$ in the *as-model* is lower than the value we have used in previous studies of spinstars (0.6–0.8) (Chiappini et al. 2006, 2008). In addition, recent star formation simulations (Stacy et al. 2011, 2013) support high rotation velocities compatible with higher $v_{\rm ini}/v_{\rm crit}$ ratios. Furthermore, the current uncertainties in the $^{17}{\rm O}(\alpha,\gamma)$ rate are still large. The adopted value of one tenth of the standard one is well within both the theoretical and recent experiments uncertainties.

We do not have a fully computed grid for these parameters, but we did scale the previous yields guided by the results obtained with these parameters for a 25 $M_{\odot}$ of $Z = 10^{-5}$ by Frischknecht et al. (2012, cf. in their paper Table 2), and applied the same factor to all the masses at $Z = 10^{-5}$, as shown in Fig. 4. Again, for this *fs-model*, in addition to the *s*-process in spinstars, we took the contribution by our empirical standard *r*-process into account.

Finally we note that Frischknecht et al. (2012) only provide the pre-supernovae yields. However, the supernova shock only affects the bottom of the carbon shell and not the whole *s*-process-rich region. The *s*-process takes place at the end of core He-burning, and the start of shell carbon burning. At low *Z*, as explained in Frischknecht et al. (2012), the contribution from carbon shell burning is very small because of the strong neutron poisons during this phase. The composition of the *s*-process-rich layers are thus set by the end of He-burning, and very little happens during the advanced stages at very low *Z*. As a consequence the bulk of the *s*-process-rich material remains almost unaffected by the SN explosion (also the case of light elements such as C, N, and O – see Woosley et al. 2002). A more recent study by

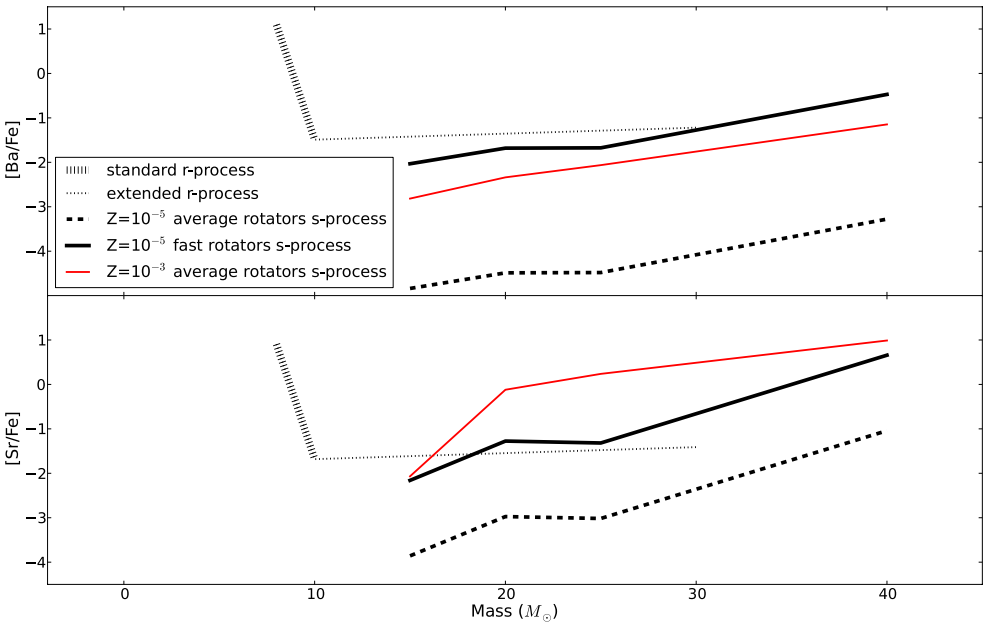

Fig. 4. Yields used, normalized to the solar (Grevesse et al. 2010), for the ratios of [Ba/Fe] and [Sr/Fe], as a function of the stellar mass and the metallicities.

Tur et al. (2009) shows that certain isotopes can be affected by both explosive nucleosynthesis and also shell mergers possibly taking place during the early collapse. These changes will, however, not affect elemental ratios like [Sr/Ba] and the conclusions of our paper.

5. Results

Our main results are summarized In Fig. 5. We started by analyzing the results of the *r-model* (upper panel), which only assumes the contribution from massive stars via our empirical *r*-process yields. The spread obtained by this model matches the dispersion of [Ba/Fe] (upper, left panel), confirming that the hypothesis of a contribution by two distinct sites seems to be a good one to explain the data. In the particular case of this model, the two sites of production are illustrated by a standard *r*-process that takes place in the lower mass range of the massive stars, and an extended *r*-process taking place in more massive stars. The first one is assumed to be much more efficient (larger quantities of ejected material) than the second.

We also consider the match with the observed [Sr/Fe] obtained by the same model to be a good match, especially at very low metallicities, because more than 80% of the stars below [Fe/H] < -3 are within the model results. Since the Sr yields adopted here are obtained just by using the Ba/Sr ratio matching the observed solar system *r*-process (Sneden et al. 2008), the results for this ratio are simply constant with metallicity (as shown in the upper right panel). This suggests that some other physical process, taking place in the same mass range as what we call extended *r*-process might be contributing to producing part of the Sr and Ba in the very early Universe (since the scatter is larger between metallicities −2.5 and −3.5). In other words, the *r-model* is useful for highlighting what we are trying to solve in the present work.

We now turn to the results obtained with our *as-model* (see Table 1 and Fig. 5, second row), and see the impact of the *s*-process production of Ba and Sr by rotating massive stars on the halo chemical evolution. In this case we added a rather conservative *s*-process production from rotating stars, and turned off the contribution of what we have called extended *r*-process. The results for [Ba/Fe] and [Sr/Fe] are not completely satisfactory because the model cannot reproduce the low [Ba/Fe] ratios observed in extremely metal-poor stars with [Fe/H] < -3 (left and middle panels of the second row). This happens because this rather conservative model does not predict enough Sr and, particularly, Ba (this can be seen in Fig. 4 by comparing the stellar yields of the extended *r*-process – dotted line – with the yields of the *as-model* at $Z = 10^{-5}$ – dashed line).

Despite the shortcomings described above, the interesting result of this model resides in the [Sr/Ba] plot (second row, right panel), where it is clear that this new process produces an overabundance and creates a spread in [Sr/Ba] at [Fe/H] ~ -3. From this, one can conclude that the *s*-process produced in fast-rotating massive stars seems to act in the correct direction. Nevertheless, these results are affected by the ratio of the yields of Sr and Ba predicted by this specific stellar evolution model (similar to model B1 of Frischknecht et al. 2012). These prescriptions produce [Sr/Ba] > 2, whereas the EMP stars show [Sr/Ba] ~ 1.5 at the maximum.

Finally for the *fs-model* (Fig. 5, bottom panels), where we adopted less conservative stellar models predicting even greater *s*-process enrichment (essentially due to a higher $v_{\rm ini}/v_{\rm crit}$ and a lower $^{17}{\rm O}(\alpha,\gamma)$ reaction rate similar to the model B4 of Frischknecht et al. 2012 – see Sect. 4.2), the theoretical predictions and observations show striking agreement. This model not only reproduces the [Ba/Fe] and [Sr/Fe] scatter closely (left and middle bottom panels), but can also account for the observed [Sr/Ba] spread (right bottom panel), at the correct metallicity interval. This shows that with a less conservative production of *s*-process in fast-rotating massive stars (as is the case in the *fs-model*), this process could play the same role as our extended *r*-process in the *r-model*. In addition, it shows that a standard *r*-process (taking place in the lower mass range of the massive stars) enters into play with a weight that increases as the metallicity increases (still in the very metal-poor range).

In the scenario of the *fs-model*, the stars with high [Sr/Ba] abundances should show the pollution by the *s*-process in spinstars. These stars should therefore present a high value of the even/odd isotopes of Ba (as typical of an *s*-process). Interestingly, the pioneering measurements of Ba isotopes in

Table 1. Nucleosynthesis prescriptions for the three cases.

Model name	Panels in Fig. 5	*s*-process	*r*-process
r-	Upper	No *s*-process from massive stars	Standard + extended *r*-process site (8–30 $M_\odot$)
as-	Middle	Average rotators ($v_{\rm ini}/v_{\rm critic}$ = 0.4)	Standard *r*-process site (8–10 $M_\odot$)
fs-	Lower	Fast rotators ($v_{\rm ini}/v_{\rm critic}$ = 0.5) and 1/10 for ^{17}O(α,γ) reaction rate	Standard *r*-process site (8–10 $M_\odot$)

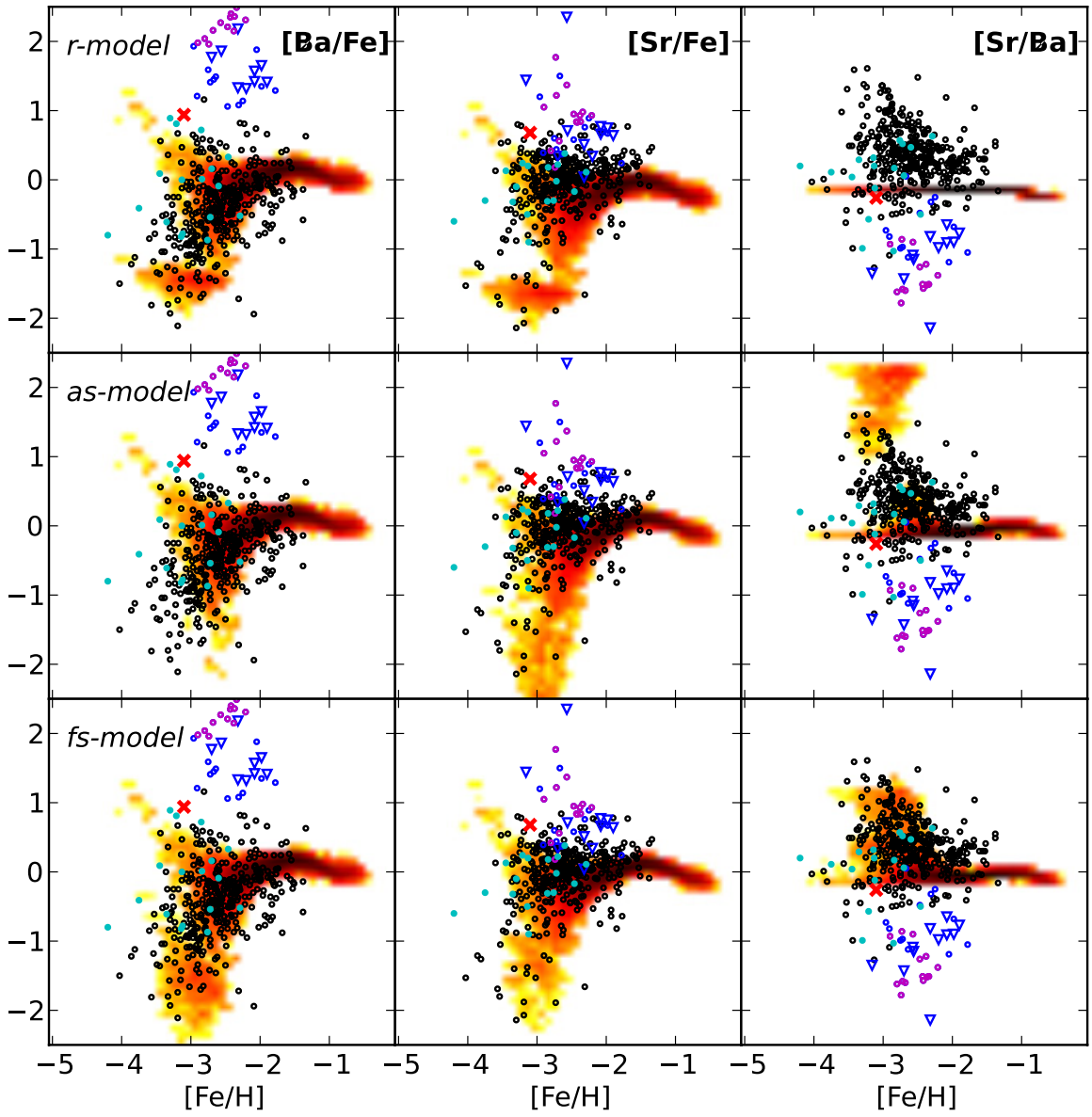

Fig. 5. On *the left* [Ba/Fe], in *the center* [Sr/Fe], on *the right* [Sr/Ba], vs. [Fe/H]. *Upper*, *center*, and *lower panels* for "*r*-", "as-", and "fs-"models respectively. The density plot is the distribution of simulated long-living stars for our models; the density is on a log scale, normalized to the peak of the distribution (see bar over the Fig. 2 for the color scale). Superimposed, we show the abundances ratios for halo stars (data from Frebel 2010). The symbols are the same as in Fig. 3.

six EMP stars by Gallagher et al. (2010, 2012) have shown exactly the feature we predict with the above models, namely, a high level of even isotopes compatible with an *s*-process production. It is important to note that four of these stars, with Sr abundances available in literature, present high [Sr/Ba] ratios, excluding AGB pollution; for the remaning two stars, a similar conclusion is supported by the *Y* abundance. We are aware that even with the highest resolution and signal-to-noise available, the measurement of the ratio of odd-to-even isotopes of Ba could still suffer from large uncertainties (such as broadening of the studied lines due to the differential hyperfine splitting of its isotopes). More measurements would be needed to confirm our suggestions. We stress, however, that at present, only our scenario can explain these observations.

In Fig. 6, we plot the [Sr/Ba] vs. [Ba/Fe] similarly to the plots in the works by Montes et al. (2007) and François et al. (2007). Our model can reproduce the peculiar behavior seen in EMP stars, namely, a high ratio of [Sr/Ba] at low [Ba/Fe] and

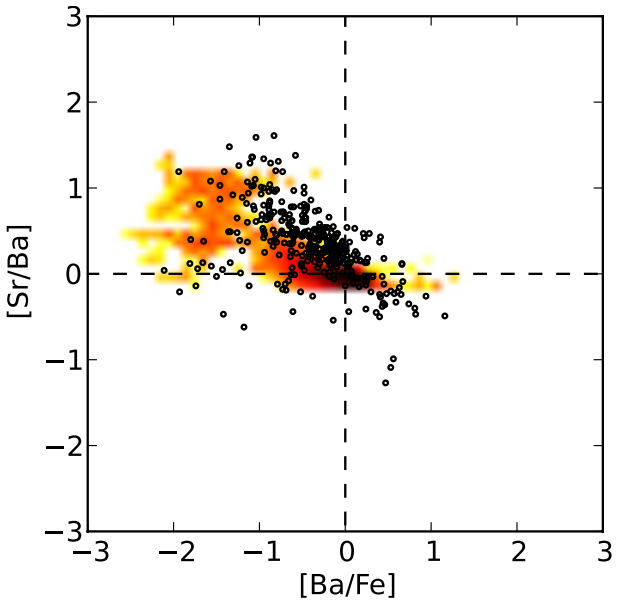

Fig. 6. [Sr/Ba] vs. [Ba/Fe], the density plot is the distribution of simulated long-living stars for *fs-model*. The density is on a log scale, normalized to the peak of the distribution (see bar over the Fig. 2 for the color scale). Superimposed on the density plot, we show the abundances ratios only for normal halo stars (data from Frebel 2010).

the correct amount of scatter. This behavior in the model is determined by the fact that by including the *s*-process production in spinstars, we are able to decouple the sites responsible for the *r*-process process enrichment (8–10 $M_{\odot}$), from the producers of *s*-process in the early Universe (i.e. the most massive spinstars, which are responsible for the largest contributions). In volumes where the most massive stars contribute more, the production of *s*-process will be important, and the [Sr/Ba] ratios will be high. However, in this case the net enrichment in Ba and Sr will be low (due to the low yields produced by this process), which will then lead to low [Ba/Fe] and [Sr/Fe] ratios. On the other hand, in volumes where the contribution of the less massive stars is greater, the standard *r*-process will tend to produce higher levels of [Ba/Fe] and [Sr/Fe] enrichment, whereas the [Ba/Sr] will tend to be lower. The different mixtures of these two limits is dictated by the stochasticity of the star formation rate of each independent volume, which then lead to the observed spread.

6. Discussions and conclusions

We have developed an inhomogeneous chemical evolution model for the halo with the aim of explaining the observed scatter (or lack of) in the abundance ratios of key chemical elements in very metal-poor stars. The models presented here serve as a test-bench to study the different nucleosynthetic prescriptions proposed by different stellar evolution groups. The goal is to identify the most promising stellar yields for key abundance ratios (in this case neutron capture elements) to then be implemented in cosmological simulations (a project that we are already pursuing). This step is crucial to avoid spending unnecessary CPU time with models that do not meet the minimum requirements set by a first comparison with observations. In addition, the comparison of our model predictions with observations is very useful for offering additional constraints to the theoretical nucleosynthesis predictions, which are still very uncertain for these elements.

Our main results and conclusions are summarized below.

- We first showed that it is possible to reproduce the observed spread of [Ba/Fe] and [Sr/Fe] and the simultaneous lack of scatter in the α-elements in EMP stars with an inhomogeneous chemical evolution model, if we assume a production of neutron capture elements coming from: a) a relatively rare, but efficient, site of production (here illustrated by a contribution of stars in the 8–10 $M_{\odot}$ mass range), and b) a second site of production, which is less efficient when producing lower amounts of neutron capture (here illustrated with a contribution from stars in the 10–40 $M_{\odot}$ mass range). More important, we show that despite the good agreement with the observed spread of [Ba/Fe] and [Sr/Fe], an extra process is needed to explain the observed [Sr/Ba] scatter.
- The presence of *r*-process-rich stars, with a common strong *r*-process signature, is an observational constraint for the first site of production: only if this site produces strong enhancement in relatively rare events can the chemical evolution model then provide an explanation for the *r*-process-rich stars. Here we show that keeping this first site of production fixed, but adding the contribution to the neutron capture elements by fast-rotating massive stars (now considered as the second site of production), then it is possible to create scatter in the ratio of [Sr/Ba], as observed.
- In particular, when considering stellar models for fast-rotating massive stars that are less conservative in their assumptions (what we call here spinstar *s*-process models), we are then able, for the first time to our knowledge, to reproduce simultaneous the [α/Fe], [Sr/Fe], [Ba/Fe], and [Sr/Ba] trends and scatter observed in halo stars with an inhomogenous chemical evolution model. Although the proposition that the scatter in the observed spread between heavy and light neutron capture elements in EMP stars could be due to the contribution of spinstars had been made before (Chiappini et al. 2011), but here we show quantitative estimates that seem to confirm this hypothesis. In this elegant solution, we are able to explain the results with just two different sites of production for Sr and Ba, without requiring more complicated scenarios.
- The above solution is based on the existence of spinstars in the early Universe. Indeed, this is not the first chemical signature to reveal the importance of fast-rotating massive stars in the early chemical enrichment of the Galaxy. On the contrary, very old halo stars were previously found to show at least four other abundance anomalies, which rotating models of massive stars can successfully account for: rise in N/O and C/O (Chiappini et al. 2006), low $^{12}C/^{13}C$ (Chiappini et al. 2008) and a primary-like evolution of Be and B (Prantzos 2012). What we provide here is a fifth independent signature: an early enrichment of the Universe in *s*-process elements.
- Our model thus predicts that stars with high [Sr/Ba] abundances should show the pollution by the *s*-process in spinstars. These stars should therefore present a high value of the even/odd isotopes of Ba (typical of an *s*-process). We are aware that even with the highest resolution and signal-to-noise available, the measurement of the ratio of odd-to-even isotopes of Ba could still suffer from large uncertainties, but measurements of this ratio would be needed to confirm our suggestions.
- Our results also show that to reconcile the model to the observations, we need an *r*-process site of production decoupled from the one of *s*-process. We assumed here the most straightforward solution, which is to consider two different

mass ranges for the two processes, but other solutions providing a large amount of *r*-process production in only a fraction (roughly 15%) of the massive stars would be equally valid, as in the case of magnetorotationally driven supernovae (Winteler et al. 2012).

– At variance with suggestions so far in the literature of a possible second *r*-process or weak *r*-process to explain the observations, the production of *s*-process in fast-rotating massive stars, does predict an enrichment in Ba (although not as strong as for Sr), and a negligible production of Eu. Another natural outcome of our model is thus the production of a small spread (∼0.3 dex) in the ratio of [Eu/Ba], which a scenario involving two different *r*-processes cannot reproduce. The [Eu/Ba] spread is observed in stars with [Fe/H] ~ -3, although more data is needed to probe this additional, valuable observational constraint.

We are aware that the recent simulations of star formation in the early universe find that most of the first stars are formed in binary systems (Stacy et al. 2013). However, binary stars, just like single stars, should also experience rotation-induced mixing that is the key property for producing of *s*-process in spinstars (as shown for the extreme case of long GRB progenitors by Cantiello et al. (2007). Indeed, the above simulations do predict the first stars to have high initial rotational velocities.

As a final comment we notice that, intriguingly, the CEMP-no stars appear indistinguishable on the basis of the neutron capture elements from normal EMP stars. In Cescutti & Chiappini (2010), our inhomogenous model with fast-rotating massive stars was not able to account for the C/O and N/O ratios in the same CEMP-no stars. As mentioned in Cescutti & Chiappini (2010), the explanation can reside in a pollution by a process that produces C in a non standard chemical enrichment fashion (i.e. without mixing with all the surrounding ISM). That no strong *s*-process signature is observed in these stars could support the scenario described in Meynet et al. (2010), in which a fast-rotator star enriches low-mass stars belonging to its forming stellar cluster through its stellar wind, highly enriching them in C, without strong dilution by the ISM. In this case, no *s*-process can pollute these low-mass stars because the *s*-process in fast-rotating massive stars are not removed by wind, because not present on the surface. However, we cannot exclude a scenario in which also CEMP-no are formed by an AGB companion with a dimmed production of *s*-process (although most of the CEMP-no appear to be single stars at the present time, see Norris et al. 2013).

Acknowledgements. We thank the two referees, one theoretical and one observational, for the helpful suggestions and comments that have improved this manuscript. R. Hirschi acknowledges support from the World Premier International Research Center Initiative (WPI Initiative), MEXT, Japan; R. Hirschi and C. Chiappini acknowledge support from the Eurogenesis EUROCORE program. The research leading to these results has received funding from the European Research Council under the European Union's Seventh Framework Program (FP/2007-2013) / ERC Grant Agreement N. 306901.

References

Abel, T., Bryan, G. L., & Norman, M. L. 2002, Science, 295, 93
Aoki, W., Ando, H., Honda, S., et al. 2002, PASJ, 54, 427
Aoki, W., Honda, S., Beers, T. C., et al. 2005, ApJ, 632, 611
Aoki, W., Frebel, A., Christlieb, N., et al. 2006, ApJ, 639, 897
Aoki, W., Honda, S., Beers, T. C., et al. 2007, ApJ, 660, 747
Arcones, A., & Montes, F. 2011, ApJ, 731, 5
Arcones, A., Janka, H.-T., & Scheck, L. 2007, A&A, 467, 1227
Argast, D., Samland, M., Thielemann, F.-K., & Gerhard, O. E. 2002, A&A, 388, 842
Argast, D., Samland, M., Thielemann, F.-K., & Qian, Y.-Z. 2004, A&A, 416, 997
Arlandini, C., Käppeler, F., Wisshak, K., et al. 1999, ApJ, 525, 886
Arnould, M., Goriely, S., & Takahashi, K. 2007, Phys. Rep., 450, 97
Balcells, M., Benn, C. R., Carter, D., et al. 2010, in SPIE Conf. Ser., 7735
Barbuy, B., Zoccali, M., Ortolani, S., et al. 2009, A&A, 507, 405
Barklem, P. S., Christlieb, N., Beers, T. C., et al. 2005, A&A, 439, 129
Bisterzo, S., Gallino, R., Straniero, O., Cristallo, S., & Käppeler, F. 2012, MNRAS, 422, 849
Bonifacio, P., Spite, M., Cayrel, R., et al. 2009, A&A, 501, 519
Bonifacio, P., Sbordone, L., Caffau, E., et al. 2012, A&A, 542, A87
Boyd, R. N., Famiano, M. A., Meyer, B. S., et al. 2012, ApJ, 744, L14
Bromm, V., & Larson, R. B. 2004, ARA&A, 42, 79
Bromm, V., & Yoshida, N. 2011, ARA&A, 49, 373
Bromm, V., Coppi, P. S., & Larson, R. B. 1999, ApJ, 527, L5
Burbidge, E. M., Burbidge, G. R., Fowler, W. A., & Hoyle, F. 1957, Rev. Mod. Phys., 29, 547
Caffau, E., Bonifacio, P., François, P., et al. 2011, Nature, 477, 67
Cameron, A. G. W. 2003, ApJ, 587, 327
Cantiello, M., Yoon, S.-C., Langer, N., & Livio, M. 2007, A&A, 465, L29
Caughlan, G. R., & Fowler, W. A. 1988, Atomic Data and Nuclear Data Tables, 40, 283
Cayrel, R., Hill, V., Beers, T. C., et al. 2001, Nature, 409, 691
Cayrel, R., Depagne, E., Spite, M., et al. 2004, A&A, 416, 1117
Cescutti, G. 2008, A&A, 481, 691
Cescutti, G., & Chiappini, C. 2010, A&A, 515, A102
Cescutti, G., François, P., Matteucci, F., Cayrel, R., & Spite, M. 2006, A&A, 448, 557
Chiappini, C. 2012, Red Giant Stars: Probing the Milky Way Chemical Enrichment, eds. A. Miglio, J. Montalbán, & A. Noels, 147
Chiappini, C., Hirschi, R., Meynet, G., et al. 2006, A&A, 449, L27
Chiappini, C., Ekström, S., Meynet, G., et al. 2008, A&A, 479, L9
Chiappini, C., Frischknecht, U., Meynet, G., et al. 2011, Nature, 472, 454
Christlieb, N., Bessell, M. S., Beers, T. C., et al. 2002, Nature, 419, 904
Christlieb, N., Schörck, T., Frebel, A., et al. 2008, A&A, 484, 721
Clark, P. C., Glover, S. C. O., Smith, R. J., et al. 2011, Science, 331, 1040
Cohen, J. G., Christlieb, N., McWilliam, A., et al. 2008, ApJ, 672, 320
Cowan, J. J., Sneden, C., Burles, S., et al. 2002, ApJ, 572, 861
de Jong, R. S., Bellido-Tirado, O., Chiappini, C., et al. 2012, in SPIE Conf. Ser., 8446
Eisenstein, D. J., Weinberg, D. H., Agol, E., et al. 2011, AJ, 142, 72
Fabbian, D., Nissen, P. E., Asplund, M., Pettini, M., & Akerman, C. 2009, A&A, 500, 1143
Farouqi, K., Kratz, K.-L., Mashonkina, L. I., et al. 2009, ApJ, 694, L49
Ferrara, A. 2012, in AIP Conf. Ser. 1480, eds. M. Umemura, & K. Omukai, 317
François, P., Matteucci, F., Cayrel, R., et al. 2004, A&A, 421, 613
François, P., Depagne, E., Hill, V., et al. 2007, A&A, 476, 935
Frebel, A. 2010, Astron. Nachr., 331, 474
Frebel, A., Aoki, W., Christlieb, N., et al. 2005, Nature, 434, 871
Frebel, A., Collet, R., Eriksson, K., Christlieb, N., & Aoki, W. 2008, ApJ, 684, 588
Freeman, K., & Bland-Hawthorn, J. 2002, ARA&A, 40, 487
Freiburghaus, C., Rosswog, S., & Thielemann, F.-K. 1999, ApJ, 525, L121
Frischknecht, U., Hirschi, R., & Thielemann, F.-K. 2012, A&A, 538, L2
Gallagher, A. J., Ryan, S. G., García Pérez, A. E., & Aoki, W. 2010, A&A, 523, A24
Gallagher, A. J., Ryan, S. G., Hosford, A., et al. 2012, A&A, 538, A118
Goriely, S., Bauswein, A., & Janka, H.-T. 2011, ApJ, 738, L32
Greif, T. H., Springel, V., White, S. D. M., et al. 2011, ApJ, 737, 75
Greif, T. H., Bromm, V., Clark, P. C., et al. 2012, MNRAS, 424, 399
Grevesse, N., Asplund, M., Sauval, A. J., & Scott, P. 2010, Ap&SS, 328, 179
Hayek, W., Wiesendahl, U., Christlieb, N., et al. 2009, A&A, 504, 511
Honda, S., Aoki, W., Kajino, T., et al. 2004, ApJ, 607, 474
Ishimaru, Y., & Wanajo, S. 1999, ApJ, 511, L33
Ivans, I. I., Sneden, C., James, C. R., et al. 2003, ApJ, 592, 906
Ivans, I. I., Simmerer, J., Sneden, C., et al. 2006, ApJ, 645, 613
Jaikumar, P., Meyer, B. S., Otsuki, K., & Ouyed, R. 2007, A&A, 471, 227
Joggerst, C. C., & Whalen, D. J. 2011, ApJ, 728, 129
Käppeler, F., Gallino, R., Bisterzo, S., & Aoki, W. 2011, Rev. Mod. Phys., 83, 157
Karlsson, T., & Gustafsson, B. 2005, A&A, 436, 879
Karlsson, T., Bromm, V., & Bland-Hawthorn, J. 2011 [arXiv:1101.4024]
Keller, S. C., Schmidt, B. P., Bessell, M. S., et al. 2007, PASA, 24, 1
Kitaura, F. S., Janka, H.-T., & Hillebrandt, W. 2006, A&A, 450, 345
Kobayashi, C., Karakas, A. I., & Umeda, H. 2011, MNRAS, 414, 3231
Korobkin, O., Rosswog, S., Arcones, A., & Winteler, C. 2012, MNRAS, 426, 1940
Lai, D. K., Johnson, J. A., Bolte, M., & Lucatello, S. 2007, ApJ, 667, 1185

Lai, D. K., Bolte, M., Johnson, J. A., et al. 2008, ApJ, 681, 1524
Li, H. N., Christlieb, N., Schörck, T., et al. 2010, A&A, 521, A10
Lucatello, S., Beers, T. C., Christlieb, N., et al. 2006, ApJ, 652, L37
Lugaro, M., Karakas, A. I., Stancliffe, R. J., & Rijs, C. 2012, ApJ, 747, 2
Maeder, A., & Meynet, G. 1989, A&A, 210, 155
Maeder, A., & Meynet, G. 2012, Rev. Mod. Phys., 84, 25
Masseron, T., van Eck, S., Famaey, B., et al. 2006, A&A, 455, 1059
Masseron, T., Johnson, J. A., Plez, B., et al. 2010, A&A, 509, A93
McWilliam, A. 1998, AJ, 115, 1640
McWilliam, A., Preston, G. W., Sneden, C., & Searle, L. 1995, AJ, 109, 2757
Meynet, G., Ekström, S., Maeder, A., et al. 2008, in First Stars III, eds. B. W. O'Shea, & A. Heger, AIP Conf. Ser., 990, 212
Meynet, G., Hirschi, R., Ekstrom, S., et al. 2010, A&A, 521, A30
Montes, F., Beers, T. C., Cowan, J., et al. 2007, ApJ, 671, 1685
Muijres, L., Vink, J. S., de Koter, A., et al. 2012, A&A, 546, A42
Norris, J. E., Yong, D., Bessell, M. S., et al. 2013, ApJ, 762, 28
Pignatari, M., Gallino, R., Meynet, G., et al. 2008, ApJ, 687, L95
Prantzos, N. 2012, A&A, 542, A67
Preston, G. W., Sneden, C., Thompson, I. B., Shectman, S. A., & Burley, G. S. 2006, AJ, 132, 85
Raiteri, C. M., Gallino, R., & Busso, M. 1992, ApJ, 387, 263
Roederer, I. U. 2013, AJ, 145, 26
Roederer, I. U., Frebel, A., Shetrone, M. D., et al. 2008, ApJ, 679, 1549
Roederer, I. U., Cowan, J. J., Karakas, A. I., et al. 2010, ApJ, 724, 975
Scalo, J. M. 1986, Fund. Cosmic Phys., 11, 1
Schörck, T., Christlieb, N., Cohen, J. G., et al. 2009, A&A, 507, 817
Siess, L. 2007, A&A, 476, 893
Siess, L. 2010, A&A, 512, A10
Simmerer, J., Sneden, C., Cowan, J. J., et al. 2004, ApJ, 617, 1091
Sneden, C., McWilliam, A., Preston, G. W., et al. 1996, ApJ, 467, 819
Sneden, C., Cowan, J. J., Lawler, J. E., et al. 2003, ApJ, 591, 936
Sneden, C., Cowan, J. J., & Gallino, R. 2008, ARA&A, 46, 241
Spite, M., Cayrel, R., Plez, B., et al. 2005, A&A, 430, 655
Spite, M., Cayrel, R., Hill, V., et al. 2006, A&A, 455, 291
Stacy, A., Bromm, V., & Loeb, A. 2011, MNRAS, 413, 543
Stacy, A., Greif, T. H., Klessen, R. S., Bromm, V., & Loeb, A. 2013, MNRAS, 431, 1470
Takahashi, K., Witti, J., & Janka, H.-T. 1994, A&A, 286, 857
Thielemann, F.-K., Arcones, A., Käppeli, R., et al. 2011, Prog. Part. Nucl. Phys., 66, 346
Thompson, T. A. 2003, ApJ, 585, L33
Thornton, K., Gaudlitz, M., Janka, H.-T., & Steinmetz, M. 1998, ApJ, 500, 95
Travaglio, C., Galli, D., Gallino, R., et al. 1999, ApJ, 521, 691
Travaglio, C., Galli, D., & Burkert, A. 2001, ApJ, 547, 217
Travaglio, C., Gallino, R., Arnone, E., et al. 2004, ApJ, 601, 864
Truran, J. W. 1981, A&A, 97, 391
Tsujimoto, T., Shigeyama, T., & Yoshii, Y. 1999, ApJ, 519, L63
Tumlinson, J. 2010, ApJ, 708, 1398
Tur, C., Heger, A., & Austin, S. M. 2009, ApJ, 702, 1068
Wanajo, S., Nomoto, K., Janka, H.-T., Kitaura, F. S., & Müller, B. 2009, ApJ, 695, 208
Wanajo, S., Janka, H.-T., & Müller, B. 2011, ApJ, 726, L15
Wasserburg, G. J., Busso, M., & Gallino, R. 1996, ApJ, 466, L109
Westin, J., Sneden, C., Gustafsson, B., & Cowan, J. J. 2000, ApJ, 530, 783
Winteler, C., Käppeli, R., Perego, A., et al. 2012, ApJ, 750, L22
Woosley, S. E., Wilson, J. R., Mathews, G. J., Hoffman, R. D., & Meyer, B. S. 1994, ApJ, 433, 229
Woosley, S. E., Heger, A., & Weaver, T. A. 2002, Rev. Mod. Phys., 74, 1015
Yanny, B., Rockosi, C., Newberg, H. J., et al. 2009, AJ, 137, 4377
Yong, D., Norris, J. E., Bessell, M. S., et al. 2013, ApJ, 762, 27
Zhao, G., Chen, Y.-Q., Shi, J.-R., et al. 2006, Chinese J. Astron. Astrophys., 6, 265

Appendix A

We present in Fig. A.1, the results of our inhomogenous model, with and without the "extended" site for the *r*-process. Thanks to the inhomogeneous model, it is possible to highlight that if we use only the "standard" *r*-process site (left panel), most of the stars showing a low [Ba/Fe] cannot be reproduced by our model. This problem is not clear from the results of the homogeneous model because the simple line representing the homogeneous results cannot display that a negligible amount of stars are formed by the model in this area.

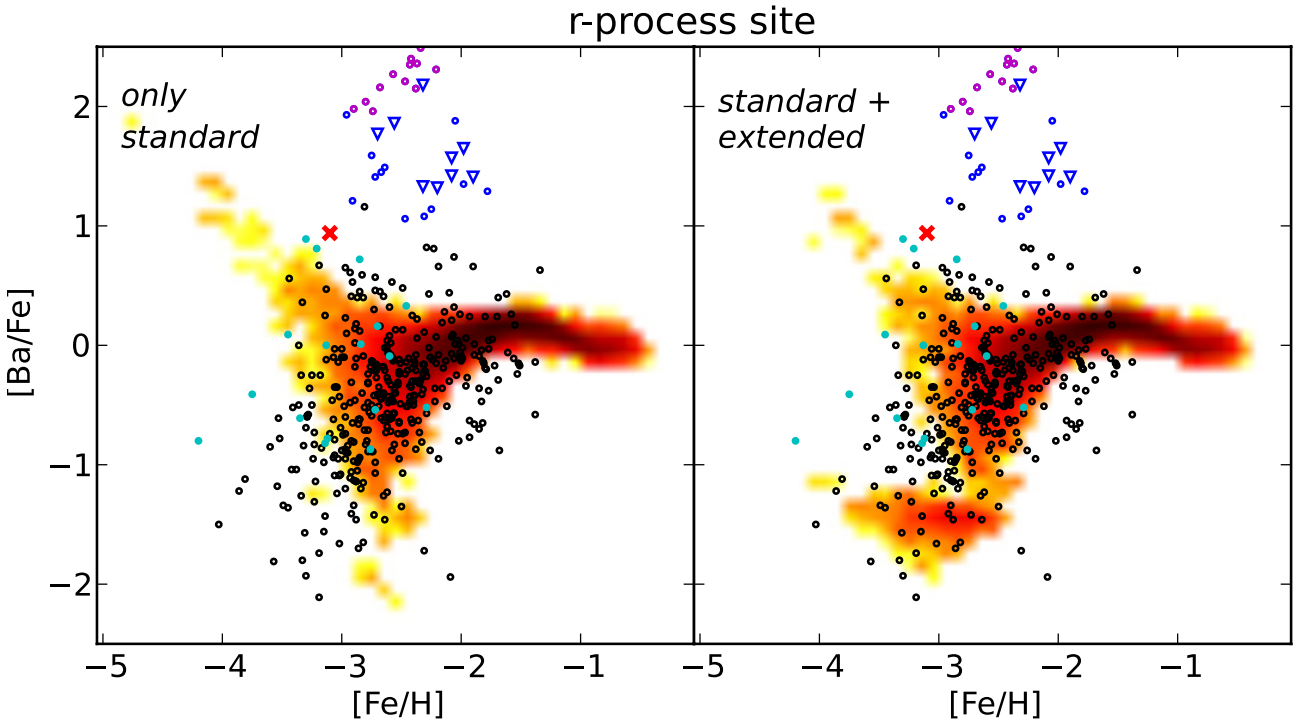

Fig. A.1. [Ba/Fe] vs. [Fe/H] results; on the left the model for an *r*-process contribution only from the "standard" site, on the right the *r-model*, where both "standard" and "extended" contributions are considered. The density plot is the distribution of simulated long-living stars for our models; the density is on a log scale, normalized to the peak of the distribution (see bar over the Fig. 2 for the color scale). Superimposed, we show the abundances ratios for halo stars (data from Frebel 2010). The symbols are the same as in Fig. 3.